Tetrahedron 65 (2009) 7213–7219

Contents lists available at ScienceDirect

Tetrahedron

journal homepage: www.elsevier.com/locate/tet

A close inspection of Ag(I) coordination to molecular baskets. A study of solvation and guest encapsulation in solution and the solid state

Matthew Gardlik, Zhiqing Yan, Shijing Xia, Stephen Rieth, Judith Gallucci, Christopher M. Hadad, Jovica D. Badjić *

Department of Chemistry, The Ohio State University, 100 West 18th Avenue, Columbus, OH 43210, USA

A R T I C L E I N F O

Article history:
Received 21 May 2008
Received in revised form 11 July 2008
Accepted 27 November 2008
Available online 6 December 2008

Keywords:
Molecular baskets
Host–guest chemistry
Encapsulation
Silver(I) coordination

A B S T R A C T

Four molecular baskets **1**–**4**, each comprising a modular bowl-shaped platform and a set of distinctive aromatic gates, were synthesized. The gates were made to incorporate a nitrogen heteroatom at different positions, as in **2**–**4**, or without a coordinating nitrogen, as in **1** (Fig. 1). For polydentate **3** and **4**, the location of the nitrogen was revealed to have an effect on directing the basket's coordination to Ag(I) cation, and subsequent folding to enclose space. The folded geometries were shown to encompass a helical, Ag(I):**3**, or C_{3v}/C_{2v} symmetrical, Ag(I):**4**, dynamic arrangement of the gates (from density functional theory). For **2** and **1**, however, the presence of Ag(I) caused the sole formation of oligomers and the absence of coordinating interactions, respectively. Variable temperature (VT) ^{1}H and ^{19}F NMR measurements of Ag(I):**3** did not provide direct evidence for the solvation of its inner space and the encapsulation of the $BF_4{-}$ counterion. Moreover, CH_3CN or CH_3NC substrates were not found inside of Ag(I):**3**. The finding is in contrast with the behavior of Cu(I):**3**, which is known to encapsulate these guests. The intriguing guest selectivity was accounted for by small structural and electronic differences of Ag(I)/Cu(I) folded baskets. The X-ray solid-state structural studies of **2**, **3**, and **4** revealed the basket's capacity to fill its inner space with small compounds. Thus, **3** was found with an ordered molecule of chloroform, while **4** contained molecules of CH_3OH and H_2O. The basket selectivity for enclosing and positioning guests, in the solid state, was deduced to be guided by their size and weak host–guest and guest–guest noncovalent interactions.

1. Introduction

The design of dynamic receptors[1] and the study of their operational mechanisms[2] have been of a considerable interest in recent years.[3] These endeavors are inspired by nature where biological molecules mediate a synchronous formation and cleavage of covalent bonds via directed chemical processes.[4] Our approach in designing functional abiotic receptors has involved the preparation and mechanistic studies of a family of molecular baskets,[5] containing a semi-rigid and curved C_{3v} symmetrical tris-norbornadiene framework (Scheme 1 and Fig. 1). Three aromatic rings, incorporating transition metal chelating[5d] or hydrogen-bonding sites,[5a] are installed at the rim to act as folding appendages that form a 'dynamic' inner space. Importantly, the process by which the guest(s) is(are) encapsulated and trafficked to and from the basket have been revealed to be a function of the host's 'elasticity' and metal-to-ligand coordination.[5] In this study we elaborate on the propensity of four molecular baskets **1**–**4**, to coordinate Ag(I) cation (Fig. 1). Moreover, we describe the folding behavior of such hosts and their ability to encapsulate guests in solution and the solid state. The presented study will expand our knowledge of molecular trafficking and translocation in complex chemical environments.

2. Results and discussion

The preparation of baskets **1** and **3** was reported earlier.[5a–b] Compounds **2** and **4** were obtained in a reaction of tris-anhydride **5**[5a,d] with 2- and 4-(aminomethyl)pyridine, respectively (Scheme 1). In particular, basket **2** was obtained (67% yield) by condensation of the reactants in refluxing toluene. The synthesis of **4**, however, required a more polar solvent (acetic acid, 50% yield). Evidently, the condensation of tris-anhydride **5** with various amines is, in the given multivalent setting, a function of the solvent properties (acidity, polarity, etc.) and, in some cases, the presence of external pyridine.[5b] Indeed, the mechanism for the imide formation,[6] and in particular the cyclization of the intermediate amic acid, has been shown to depend on the medium acidity. This, to a degree, explains for the experimental observations, but more importantly directs

---

* Corresponding author.
E-mail address: badjic@chemistry.ohio-state.edu (J.D. Badjić).

0040-4020/$ – see front matter © 2008 Elsevier Ltd. All rights reserved.
doi:10.1016/j.tet.2008.11.098

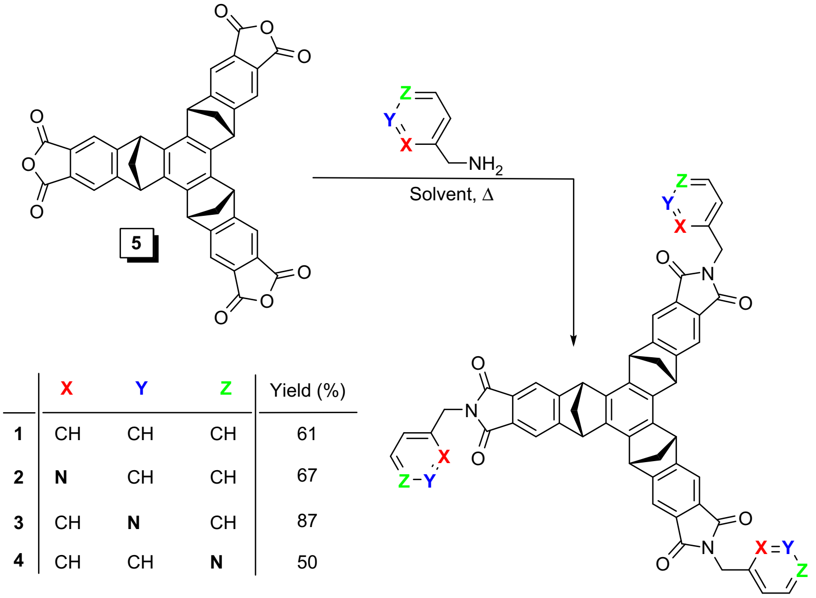

	X	Y	Z	Yield (%)
1	CH	CH	CH	61
2	**N**	CH	CH	67
3	CH	**N**	CH	87
4	CH	CH	**N**	50

Scheme 1. Chemical structures and syntheses of molecular baskets **1**–**4**.

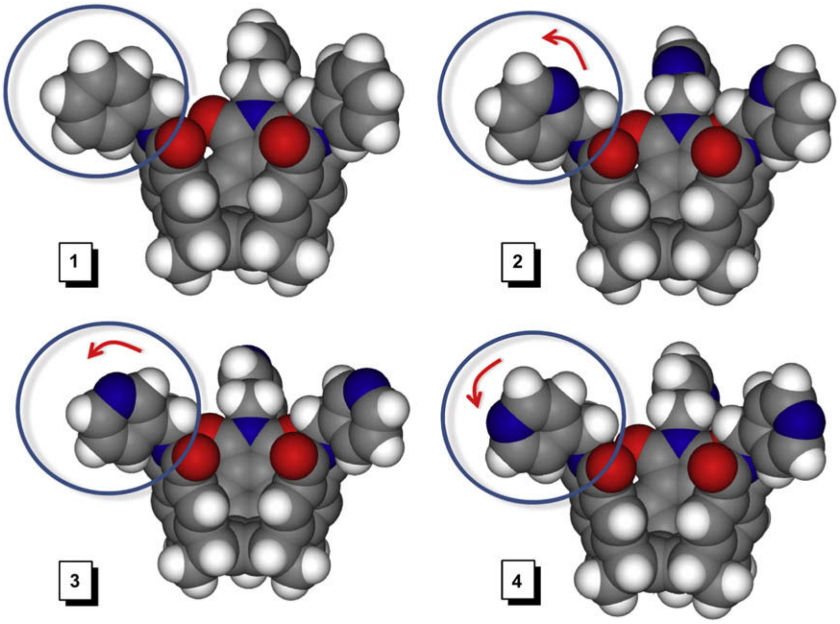

Figure 1. CPK representations of molecular baskets **1**–**4** (with and without a nitrogen heteroatom). The baskets were investigated for coordinating to Ag(I) cation in a polydentate fashion to, via folding, physically enclose space.

efforts toward completing the final step of any future basket synthesis.

Silver(I) cation has previously been shown to bind to molecular basket **3**, and to mediate its folding (Fig. 6A).[5b] On the basis of that, an intriguing question arose: how would the position of the nitrogen heteroatom in the pyridine 'flap', or perhaps its complete absence, affect the binding of the transition metal and the folding of the host? Compounds **1**–**4** (Fig. 1) were used to examine such a hypothesis.

The electron-rich bowl-shaped platform of **1**, lacking the heteroatoms in the appended flaps, can be envisaged to 'nest' Ag(I) cation. In fact, silver's ability to bind to aromatic hosts via cation-π and orbital interactions has been well documented.[7] Calixarenes and resorcinarenes, for example, employ their π-rich surface to coordinate to alkali metals[8] in the *endo*-fashion and transition metal cations (such as Rh, Ru, and Ir) in the *exo*-fashion.[9]

An incremental addition of AgOTf (29.0 mM) to a solution of **1** (2.60 mM, $CDCl_3/CD_3OD=1:1$) caused no observable change in its ^{1}H NMR spectrum (Fig. 2). In particular, the aromatic protons $\mathbf{H}_{a-c/g}$ were not affected by the presence of the silver suggesting the inferior affinity of **1** toward hosting this cation.

Subsequently, AgOTf (57.5 mM) was titrated to a solution of **2** (2.7 mM, $CDCl_3/CD_3OD=1:1$), and the coordination/assembly was followed with ^{1}H NMR spectroscopy (Fig. 3). Proton resonances in **2**, evidently, shifted to a negligible extent with the increased amounts of Ag(I) salt. More importantly, a considerable broadening of the signals for $\mathbf{H}_{a-d}$ and $\mathbf{H}_{e/f}$ protons was observed. A nearly complete disappearance of these resonances, at the equimolar

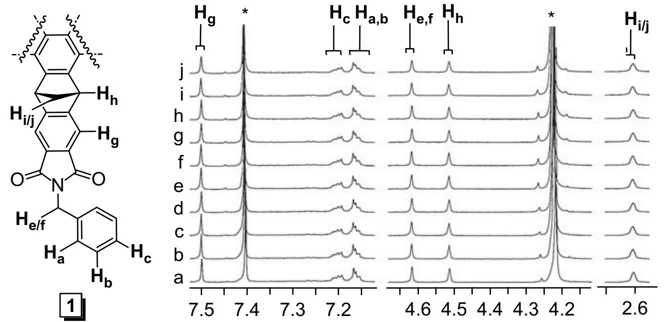

Figure 2. ^{1}H NMR spectra (500 MHz, 300 K) of **1** (2.60 mM, $CDCl_3/CD_3OD$=1:1), obtained after incremental addition of a standard solution of AgOTf (29.0 mM, $CDCl_3/CD_3OD$=1:1); the final mixture comprises (a) 0, (b) 0.2, (c) 0.4, (d) 0.5, (e) 0.7, (f) 0.8, (g) 0.9, (h) 1.0, (i) 1.2, and (j) 1.4 molar equivalents of Ag(I). The assigned ^{1}H NMR resonances are depicted in the structure of **1** on the left.

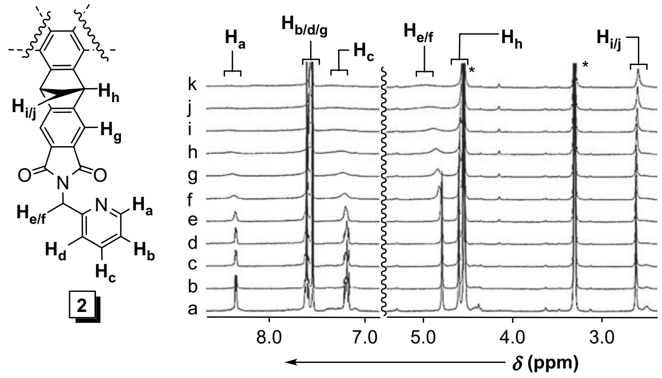

Figure 3. A series of ^{1}H NMR spectra of 2.7 mM solution of **2** (400 MHz, 300 K, $CDCl_3/CD_3OD$=1:1), recorded after a gradual addition of 57.5 mM solution of AgOTf, so that the final mixture comprises (a) 0, (b) 0.1, (c) 0.2, (d) 0.3, (e) 0.4, (f) 0.5, (g) 0.6, (h) 0.7, (i) 0.8, (j) 0.9, and (k) 1.0 molar equivalents of Ag(I). The assigned ^{1}H NMR resonances are depicted in the structure of **2** on the left.

Ag(I):**2** ratio, suggested the formation of a range of metallo-supramolecular oligomers.[10] In fact, the protons $\mathbf{H}_{a-d}$ and $\mathbf{H}_{e/f}$, belong to the dynamic (rotatable) part of the basket. They apparently resided in diverse chemical environments, upon the basket coordination to silver, to explain for the observed effects. On the contrary, the protons of the basket platform ($\mathbf{H}_{g-j}$, Fig. 3) did not 'report' on the presence of Ag(I) cations. This is consistent with their distant position from the 'flaps' and, in this particular case, robustness of the basket's 'foundation'.

When a standard solution of AgOTf (80.0 mM) was titrated into a solution of **4** (3.1 mM, CD_2Cl_2/CD_3OD=1:1), the $\mathbf{H}_a$ and $\mathbf{H}_b$ resonances moved upfield ($\Delta\delta$=0.37 and 0.03 ppm, respectively; Fig. 4). The 1:1 stoichiometric ratio of Ag(I):**4** was indicated from the break in the titration that occurs at the equimolar ratio of the two interacting species. Interestingly, the signal for the bridge protons $\mathbf{H}_{j/k}$ altered from a broad singlet in **4** to an AB type quartet in Ag(I):**4**. Arguably, the change can be ascribed to the conformational 'adjustment' of the basket platform made to accommodate Ag(I) cation at the northern part of the host. Structurally related, but more sizeable, molecular bowls[5c] have indeed been shown to comprise a semi-rigid platform capable of undergoing related 'clipping' motions.

Isothermal titration calorimetry (ITC) measurements (Fig. 5, Table 1) confirmed that the formation of Ag(I):**4** was indeed effective, K_a=2.3±0.8×10^5 M^{-1}. The experiment revealed that the assembly was driven by enthalpy ($\Delta H°$=−13.2±0.8 kcal/mol) and impeded by entropy ($\Delta S°$=−20±7 cal/mol K). The ITC entropic data do have a high degree of uncertainty, despite that the experiments were repeated multiple times; perhaps, additional minor equilibria occurred in the system and contributed to the deviations. Nonetheless, it is evident that different thermodynamic forces drive the formation of Ag(I):**4** and Ag(I):**3** folded baskets (Table 1).[5b] The calculated folding geometries of the two assemblies (density functional theory, BP86 functional)[11] can, in part, explain the observed trend (Fig. 6). That is to say, in bringing three pyridine 'flaps' together, the silver cation ends up on top of the basket, Ag(I):**4**, or is more buried inside, Ag(I):**3**. As a result, Ag(I) is more prone to the solvation in Ag(I):**4** to account for its negative folding entropy ($\Delta S°$=−20 e.u.). In the course of the coordination of Ag(I) to **3**, however, solvent molecules are less capable of approaching the silver cation and are therefore released in the assembly process ($\Delta S°$=+34 e.u.). The observed enthalpic disparity (Table 1) concurs with the above discussion, and is an indication of the enthalpy/entropy compensation effects.[12] Notably, the stabilities of polydentate Ag(I):**3** and Ag(I):**4** complexes appear to result from

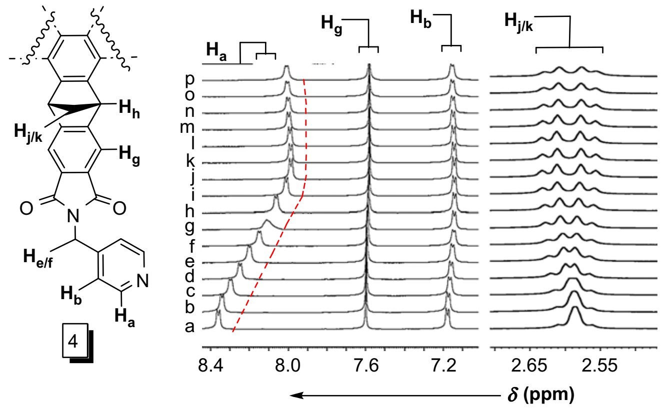

Figure 4. Selected regions of a series of ^{1}H NMR spectra of 3.1 mM solution of **4** (300 K, CD_2Cl_2/CD_3OD=1:1), recorded after a gradual addition of 80.0 mM solution of AgOTf, so that the final mixture comprises (a) 0, (b) 0.1, (c) 0.2, (d) 0.3, (e) 0.4, (f) 0.5, (g) 0.6, (h) 0.7, (i) 0.8, (j) 0.9, (k) 1.0, (l) 1.1, (m) 1.2, (n) 1.3, (o) 1.4, and (p) 1.5 molar equivalents of Ag(I). The assigned ^{1}H NMR resonances are shown in the structure of **4** on the left.

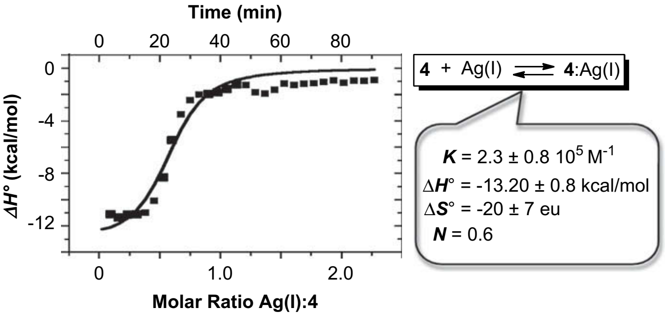

Figure 5. Isothermal titration calorimetry (ITC) data (left) for the gradual addition of a standard solution of AgOTf (0.995 mM, CH_2Cl_2/CH_3OH=9:1) to a solution of **4** (0.10 mM, CH_2Cl_2/CH_3OH=9:1) at 300 K. Computer simulated curve fitting afforded the thermodynamic parameters for the assembly (right).

Table 1
Thermodynamic parameters for the interaction of **1**–**4** with Ag(I)

Molecular basket	Stoichiometry	K_a (M^{-1})	$\Delta H°$ (kcal/mol)	$\Delta S°$ (cal/mol K)
1	No interaction	n/a	n/a	n/a
2	Aggregation	n/a	n/a	n/a
3	1:1	1.9±0.3×10^5	3.0±0.1	34.0
4	1:1	2.3±0.8×10^5	−13.2±0.8	−20

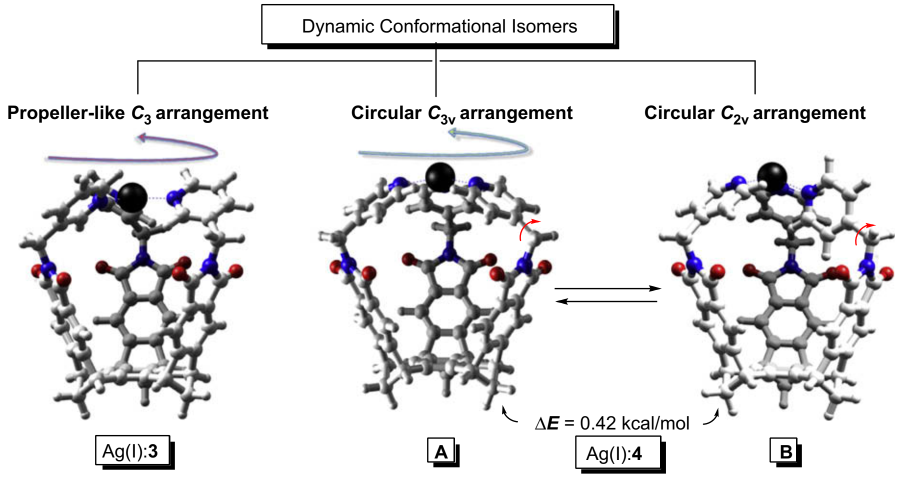

Figure 6. Energy minimized (DFT, BP86) structures of dynamic conformational isomers of folded Ag(I):**3** (left) and Ag(I):**4** (right).

chelation effects operating in their formation: in the conventional (driven by entropy) or the nonconventional fashion (driven by enthalpy).[13] Indeed, the stepwise assembly of Ag(pyridine)$_2^+$ complex was reported earlier to be thermodynamically less favorable ($K=1\times10^4$ M^{-1}).[14] The known advantage of combining mono- into multivalent ligands and gaining some stability is evident yet another time.[13]

Folded basket Ag(I):**4** has, interestingly, been calculated (BP86) to assume achiral conformations A and B (Fig. 6). The two conformers have similar stability (ΔE=0.42 kcal/mol), with conceivably a low interconversion barrier. Indeed, variable temperature ^{1}H NMR studies of Ag(I):**4** only showed broadening, but not decoalescence, of the $\mathbf{H}_{e/f}$ proton resonances at lower temperatures.[15] The gates evidently behave like revolving doors and rotate about the central 'shaft' (silver cation) with a low activation barrier.

The encapsulation of solvents, $CHCl_3$ (75 Å^3) and $CH_3C(=O)CH_3$ (72 Å^3), with Ag(I):**3** basket (137 Å^3) was investigated first. The slippage of the two compounds, through the aperture in Ag(I):**3**, was computed (PM5, CaChe) to necessitate a slight expansion of the host (Fig. 7).[16]

Accordingly, the calculations estimated a constrictive binding energy[17] of 15 kcal/mol for incorporating $CHCl_3$ and 9 kcal/mol for $CH_3C(=O)CH_3$; the computed activation barrier for the encapsulation of $CHCl_3$ was reasonable enough to expect the formation of a kinetically stable complex with Ag(I):**3**.[16] The guest exchange via gating, in which the flaps dissociate from the transition metal, requires a comparable amount of energy[18] ($\Delta G^\circ_{298}=-7.2$ kcal/mol, Table 1) and thereby presents a competitive mechanistic pathway; somewhat cooperative assembly[13] can, however, be anticipated to operate in the formation of Ag(I):**3**, to make the dissociation of the first flap an arduous task. Interestingly, variable temperature ^{1}H NMR studies of Ag(I):**3** with neat $CHCl_3$ or $CH_3C(=O)CH_3$[19] showed no sign of these molecules residing inside the folded basket.[15] Accordingly, a fast guest exchange by one of the above proposed mechanisms must be occurring to disguise the direct observation of the inner space's solvation.[19] One can also foresee solvent molecules partially occupying the inner basket space, merely protruding the host via the apertures. As $AgBF_4$ was originally used in the experiment, the counterion BF_4^- can, on the basis of its size and shape, be envisioned as a guest balancing the silver(I) charge. Variable temperature ^{19}F NMR studies of Ag(I):**3** (2.8 mM, $CD_3C(=O)CD_3/CDCl_3$=5:3) revealed a single resonance for the BF_4^- (Fig. 8). The anion stayed solely paired with the basket assembly and outside of its interior.

Silver(I) folded **3** has previously been shown to have an affinity to bind small heterocycles.[5b] The guests adopt an apical position, on the outer side of the basket, to coordinate to the transition metal. Consequently, it was discovered that CH_3CN and CH_3NC get incorporated inside Cu(I) folded **3** by coordinating the metal cation.[5d] Silver(I) is a sizeable (1.29 Å) and soft d^{10} transition metal with a known ability to bind nitriles,[20a] as well as isocyanides.[20b] It thus seemed quite reasonable to examine the encapsulation of such guests inside Ag(I):**3**, as well. When CH_3CN (100 mol equiv) was added to a solution of Ag(I):**3** (5.9 mM, $CD_3C(=O)CD_3/CDCl_3$=5:3),[15] however, there was not a typical upfield ^{1}H NMR signal for the encapsulated acetonitrile: even a great excess of the guest did not lead

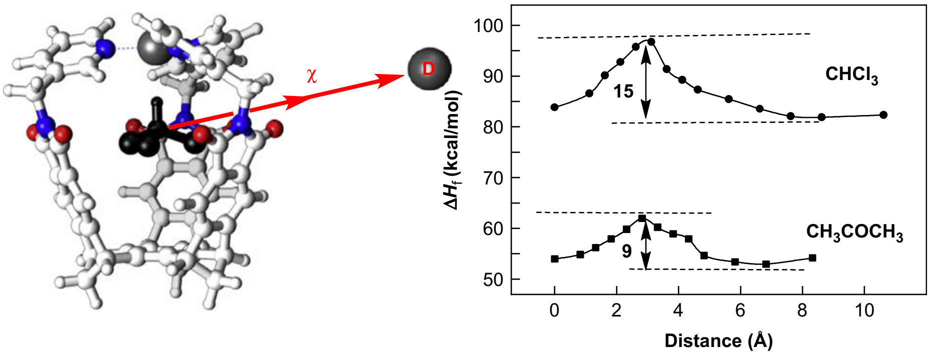

Figure 7. The reaction coordinate, χ, for the egress of $CHCl_3$ and $CH_3C(=O)CH_3$ from Ag(I):**3** (left). The computed energy profiles (PM5, CAChe), for the decomplexation of $CHCl_3$ and $CH_3C(=O)CH_3$ from Ag(I):**3**, are shown on the right.[16]

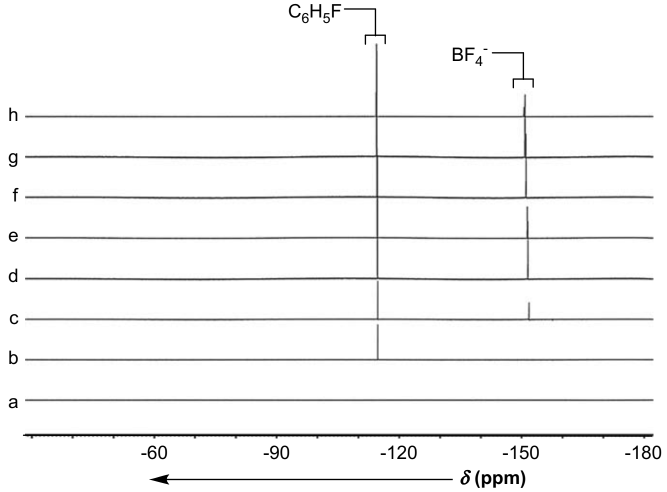

Figure 8. ^{19}F NMR spectra (400 MHz) of a solution of **3** (2.80 mM, $CD_3C(=O)CD_3$) (a) before and (b) after addition of fluorobenzene standard (C_6H_5F) at 300 K. Variable temperature ^{19}F NMR spectra (400 MHz) of Ag(I):**3** (2.80 mM, $CD_3C(=O)CD_3$) at (c) 300, (d) 283, (e) 273, (f) 258, (g) 243, and (h) 228 K.

to its encapsulation! We then used a standard solution of CH_3NC to titrate the Ag(I):**3** complex,[15] and the metal cation was gradually removed from the basket with increasing amounts of the isocyanide.[15] Likewise, imidazole and azetidine were previously shown[5b] to be capable of extracting the silver from Ag(I):**3**.

What does account for the observed conflicting host–guest behavior of the Cu(I) and Ag(I) folded baskets? One can deduce that smaller Cu(I) (0.8 Å) and bigger Ag(I) (1.29 Å) impose subtle changes on the folding geometry of the basket; somewhat different ^{1}H NMR spectra (298 K) of Cu(I) and Ag(I) folded **3** support such a notion (Fig. 9). This structural difference, in combination with the electronic character of each transition metal inside the complex, was likely expressed in the selective 'recognition' behavior of the hosts.

A single-crystal X-ray study of molecular basket **3**[15,21] revealed a C_3 symmetrical conformer with three pyridine 'flaps' pointing away from the platform (Fig. 10A). Each'flap' has a nitrogen atom located on the northern side and is residing in between two pyridines of the adjacent molecule. The crystal unit cell contains a dimer of **3**, whereby a phthalimide side 'arm' of one basket is positioned in between the neighboring two (Fig. 10B).

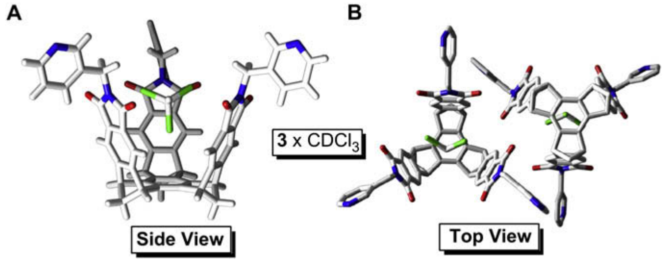

Figure 10. Stick representations (A, B) of the X-ray crystal structure of molecular basket **3**, containing an ordered molecule of $CDCl_3$.[15,21]

Remarkably, an ordered molecule of deuterated chloroform was found inside of **3**.[21] The central carbon atom, in the encapsulated $CDCl_3$, was located along the C_3 axis of the basket, with a chlorine atom directed toward the host's aromatic base. The observed host–guest order in the solid state is indeed surprising; one would anticipate that the positively polarized deuterium would be located in close proximity to the negative quadrupolar side of the bottom benzene ring. Presumably, effective packing is a decisive factor in this situation, with a bigger chlorine atom filling a fraction of the basket's inner space more effectively than a smaller deuterium. The results of the solid-state investigations also validate an earlier proposed notion that the interior of Ag(I):**3** contains a molecule of guest in the liquid phase.

Single-crystal X-ray studies of baskets **2**[24] and **4**[25] (Fig. 11)[15] revealed both compounds adopting a C_3 symmetrical conformation, which is almost identical to that observed for compound **3**. Interestingly, basket **4** had its inner space occupied with a disordered CH_3OH and an ordered molecule of H_2O (Fig. 11A). A molecule of methanol has been found distant from the C_3 axis, with its methyl group on top and the OH unit oriented inside the basket interior. Presumably, the hydroxyl proton is engaged in hydrogen bonding with the nearby oxygen atom of the encapsulated water: the oxygen–oxygen distance was found to be short, only 2.351 Å. The water molecule has its oxygen atom located on the C_3 axis, and approximately 3.6 Å from the center of each of the facing benzene rings. The water hydrogens were not resolved and therefore not added to the structure (Fig. 11A), but can be assumed to interact with the surrounding aromatic rings via non-traditional $O\text{–}H\cdots\pi$ hydrogen bonds;[26] 3.2–3.8 Å mean distance, for $X\text{–}H\cdots\pi$ contacts (X=O, N, S), has been reported for biological molecules.[26] The combined volume of CH_3OH/H_2O is 60.1 Å^3, and is similar to 74.9 Å^3 for $CHCl_3$, which itself fills the inner space of **3**. Markedly, the

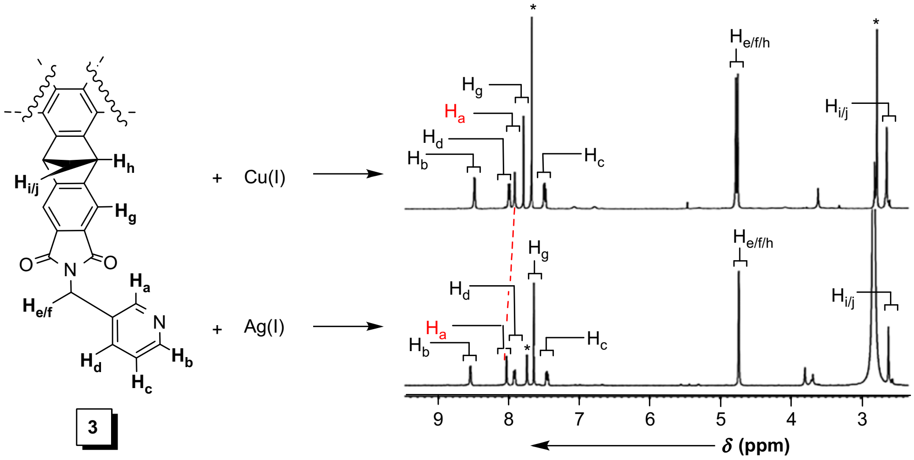

Figure 9. ^{1}H NMR spectra (400 MHz) of Ag(I):**3** (bottom) and Cu(I):**3** (top)[5d] folded molecular baskets ($CDCl_3/CD_3C(=O)CD_3$=3:5) at 298 K.

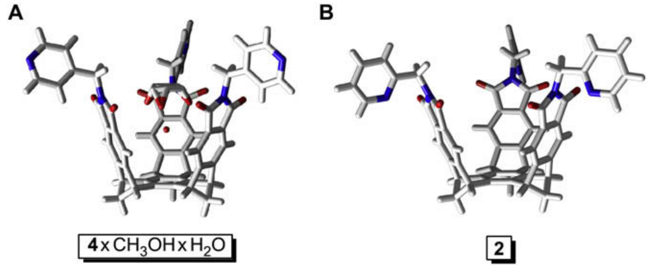

Figure 11. Stick representation of the X-ray crystal structures of **4** (A) and **2** (B) in the solid state.[15,24,25]

basket's selectivity for enclosing and positioning guests, in the solid state, is guided by their size.[27] Weak noncovalent forces augment the assembly but are evidently of secondary importance.

3. Conclusions

The transition metal mediated folding of molecular baskets is, markedly, a strategically facile and thermodynamically efficient way for generating the enclosed and dynamic space. The location of the nitrogen, within the 'flaps', is critical for creating differently folded hosts, but can also trigger the formation of extended assemblies (supramolecular polymers);[28] the code entered in the form of a slight variation of the basket structure can evidently be transferred into discrete functional behavior. Notably, the encapsulation of molecules in the metal-containing baskets bears a prominent selectivity: the Cu(I) folded host holds cylindrical ligands inside of its cavity, while the Ag(I) host is more resilient to accept guests. The observed behavior has been explained by the subtle differences in the structural, electronic, and dynamic properties of the hosts. The X-ray structural studies of baskets, lacking metal cations, have shown that small molecules indeed reside in their inner space. The recognition process and the assembly order are predominantly determined by the guest(s) size and shape, and to an extent their electrostatic characteristics.[29] The solid-state studies thus verify the solvation of the basket's inner space despite a lack of direct ^{1}H NMR spectroscopic evidence for such an occurrence.

4. Experimental

4.1. General

All chemicals were purchased from commercial sources and used as received unless stated otherwise. All solvents were dried prior to use according to standard literature protocols. Chromatography purifications were performed using silica gel 60 (Sorbent Technologies 40–75 μm, 200×400 mesh). Thin-layer chromatography (TLC) was performed on silica gel plates w/UV254 (200 μm) and chromatograms were visualized by UV-light. ^{1}H and ^{13}C NMR spectra were recorded at 400 MHz and 125 MHz, respectively, on a Bruker DPX-400 spectrometer. The spectra were referenced to the residual solvent signal(s). ^{19}F spectra were recorded on a Bruker DPX-400 spectrometer at 376 MHz and referenced to fluorobenzene (C_6H_5F) as an internal standard. Samples were prepared in $CDCl_3$, CD_2Cl_2, CD_3COCD_3, and CD_3OD purchased from Cambridge Isotope Laboratories, Inc. The chemical shift values are expressed as δ values in parts per million (ppm) and the coupling constants (J) are in hertz (Hz). The following abbreviations were used for signal multiplicities: s, singlet; d, doublet; t, triplet; m, multiplet; and br, broad. Microcalorimetric experiments were performed using an isothermal titration calorimeter (VP-ITC, MicroCal, Northampton, MA). Computer simulations (curve fittings) were performed using ORIGIN 7.0 software, adapted for ITC data analysis. The 'Single Set of Identical Sites' model was applied in all cases. Melting points are reported uncorrected. Mass Spectrometric analyses were performed on a Finnegan Orbitrap instrument.

4.2. Preparation of compounds 2 and 4

4.2.1. *Compound* **2**

Tris(anhydride) **5** (2.1 mg, 0.003 mmol) was suspended in dry toluene (2.0 mL) and 2-aminomethylpyridine (3.0 μL, 0.03 mmol) was added at room temperature. The solution was brought to reflux, after which neat pyridine (0.1 mL) was added and the reaction mixture allowed to stir at reflux (12 h). Then the solvent was removed in vacuo and the solid residue purified by column chromatography (SiO_2, CH_2Cl_2/CH_3OH=9:1) to give the desired product as a colorless solid (2.0 mg, 67%). Mp decomposition >250 °C. ^{1}H NMR (400 MHz, $CDCl_3/CD_3OD$=5:3) δ=2.425 (6H, s), 4.396 (6H, s), 4.607 (6H, s), 6.96 (6H, m), 7.397 (9H, m), 8.161 (3H, d, J=4.4 Hz). ^{13}C NMR (125 MHz, CD_2Cl_2) δ=42.59, 49.26, 66.28, 116.13, 121.15, 122.20, 130.68, 136.44, 137.94, 149.29, 156.00, 157.04, 167.97. HRMS (ESI) m/z calculated for $C_{57}H_{36}N_6O_6$: 901.2775, measured: 901.2713.

4.2.2. *Compound* **4**

Tris(anhydride) **5** (5.0 mg, 0.008 mmol) was suspended in glacial acetic acid (2.0 mL) and 4-aminomethylpyridine (5.0 μL, 0.049 mmol) was added at room temperature. The solution was brought to reflux for 12 h, after which the solvent was removed in vacuo. The solid residue was purified by column chromatography (SiO_2, CH_2Cl_2/CH_3OH=9:1) to give the desired product as a colorless solid (4.0 mg, 50%). Mp decomposition >280 °C. ^{1}H NMR (400 MHz, CD_2Cl_2/CD_3OD=5:3) δ=2.514 (6H, s), 4.527 (6H, s), 4.607 (6H, s), 7.108 (6H, d, J=6.0 Hz), 7.526 (6H, s), 8.293 (6H, dd, J_1=4.4 Hz and J_2=1.6 Hz). ^{13}C NMR (125 MHz, CD_2Cl_2/CD_3OD=5:3) δ=42.04, 68.24, 118.29, 124.85, 132.24, 139.99, 148.33, 151.18, 159.72, 169.95. (One carbon is perhaps hidden under the solvent peak at 50 ppm.) HRMS (ESI) m/z calculated for $C_{57}H_{36}N_6O_6$: 901.2775, measured: 901.2730.

Acknowledgements

This work was financially supported with funds obtained from the National Science Foundation under CHE-0716355. Computational support from the Ohio Supercomputer Center is gratefully acknowledged.

Supplementary data

Supplementary data associated with this article can be found in the online version, at doi:10.1016/j.tet.2008.11.098.

References and notes

1. Davis, A. V.; Yeh, R. M.; Raymond, K. N. *Proc. Natl. Acad. Sci. U.S.A.* **2002**, *99*, 4793–4796.
2. Palmer, L. C.; Rebek, J., Jr. *Org. Biomol. Chem.* **2004**, *2*, 3051–3059.
3. For recent examples, see: (a) Yan, Z.; Chang, Y.; Mayo, D.; Maslak, V.; Xia, S.; Badjić, J. D. *Org. Lett.* **2006**, *8*, 3697–3700; (b) Le Gac, S.; Marrot, J.; Reinaud, O.; Jabin, I. *Angew. Chem., Int. Ed.* **2006**, *45*, 3123–3126; (c) Nishioka, Y.; Yamaguchi, T.; Yoshizawa, M.; Fujita, M. *J. Am. Chem. Soc.* **2007**, *129*, 7000–7001; (d) Pluth, M. D.; Bergman, R. G.; Raymond, K. N. *Angew. Chem., Int. Ed.* **2007**, *46*, 8587–8598; (e) Yoon, H. J.; Heo, J.; Mirkin, C. A. *J. Am. Chem. Soc.* **2007**, *129*, 14182–14183; (f) Natarajan, A.; Kaanumalle, L. S.; Jockusch, S.; Gibb, B.; Gibb, C.; Turro, N. J.; Ramamurthy, V. *J. Am. Chem. Soc.* **2007**, *129*, 4132–4133; (g) Gottschalk, T.; Jaun, B.; Diederich, F. *Angew. Chem., Int. Ed.* **2007**, *46*, 260–264; (h) Huang, W.-H.; Zavalij, P. Y.; Isaacs, L. *Angew. Chem., Int. Ed.* **2007**, *46*, 7425–7427; (i) Liu, S.; Zavalij, P. Y.; Lam, Y.-F.; Isaacs, L. *J. Am. Chem. Soc.* **2007**, *129*, 11232–11241; (j) Barrett, E. S.; Dale, T. J.; Rebek, J., Jr. *J. Am. Chem. Soc.* **2008**, *130*, 2344–2350; (k) Biavardi, E.; Battistini, G.; Montalti, M.; Yebeutchou, R. M.; Prodi, L.; Dalcanale, E. *Chem. Commun.* **2008**, 1638–1640.
4. Zhang, X.; Houk, K. N. *Acc. Chem. Res.* **2005**, *38*, 379–385.

5. (a) Maslak, V.; Yan, Z.; Xia, S.; Gallucci, J.; Hadad, C. M.; Badjić, J. D. *J. Am. Chem. Soc.* **2006**, *128*, 5887–5894; (b) Yan, Z.; Xia, S.; Gardlik, M.; Seo, W.; Maslak, V.; Gallucci, J.; Hadad, C. M.; Badjić, J. D. *Org. Lett.* **2007**, *9*, 2301–2304; (c) Yan, Z.; McCracken, T.; Xia, S.; Maslak, V.; Gallucci, J.; Hadad, C. M.; Badjić, J. D. *J. Org. Chem.* **2008**, *73*, 355–363; (d) Rieth, S.; Yan, Z.; Xia, S.; Gardlik, M.; Chow, A.; Fraenkel, G.; Hadad, C. M.; Badjić, J. D. *J. Org. Chem.* **2008**, *73*, 5100—5109.
6. Wu, Z.; Ban, F.; Boyd, R. J. *J. Am. Chem. Soc.* **2003**, *125*, 3642–3648.
7. (a) Ikeda, A.; Shinkai, S. *J. Am. Chem. Soc.* **1994**, *116*, 3102–3110; (b) Munakata, L.; Wu, P.; Kuroda-Sowa, T.; Maekawa, M.; Suenaga, Y.; Sugimoto, K.; Ino, I. *J. Chem. Soc., Dalton Trans.* **1999**, 373–378.
8. Assmus, R.; Boehmer, V.; Harrowfield, J. M.; Ogden, M. I.; Richmond, W. R.; Skelton, B. W.; White, A. H. *J. Chem. Soc., Dalton Trans.* **1993**, *16*, 2427–2433.
9. (a) Staffilani, M.; Hancock, K. S. B.; Steed, J. W.; Holman, K. T.; Atwood, J. L.; Juneja, R. K.; Burkhalter, R. S. *J. Am. Chem. Soc.* **1997**, *119*, 6324–6335; (b) Lenthall, J. T.; Steed, J. W. *Coord. Chem. Rev.* **2007**, *251*, 1747–1760.
10. Iyer, P. K.; Beck, J. B.; Weder, C.; Rowan, S. J. *Chem. Commun.* **2005**, 319–321.
11. (a) Perdew, J. P. *Phys. Rev. B* **1986**, *33*, 8822–8824; (b) Becke, A. D. *Phys. Rev. A* **1998**, *38*, 3098–3100.
12. Liu, L.; Guo, Q.-X. *Chem. Rev.* **2001**, *101*, 673–695.
13. (a) Zhang, B.; Breslow, R. *J. Am. Chem. Soc.* **1993**, *115*, 9353–9354; (b) Berger, M.; Schmidtchen, F. P. *Angew. Chem., Int. Ed.* **1998**, *37*, 2694–2696; (c) Badjić, J. D.; Nelson, A.; Cantrill, S. J.; Turnbull, W. B.; Stoddart, J. F. *Acc. Chem. Res.* **2005**, *38*, 723–732; (d) Bea, I.; Gotsev, M. G.; Ivanov, P. M.; Jaime, C.; Kollman, P. A. *J. Org. Chem.* **2006**, *71*, 2056–2063.
14. Izatt, R. M.; Eatough, D.; Snow, R. L.; Christensen, J. J. *J. Phys. Chem.* **1968**, *72*, 1208–1213.
15. See Supplementary data for more details.
16. (a) Houk, K. N.; Nakamura, K.; Sheu, C.; Keating, A. E. *Science* **1996**, *273*, 627–629; (b) Sheu, C.; Houk, K. N. *J. Am. Chem. Soc.* **1996**, *118*, 8056–8070.
17. For selected examples, see: (a) Fyfe, M. C. T.; Raymo, F. M.; Stoddart, J. F. *Stimulating Concepts in Chemistry*; Wiley-VCH: Weinheim, 2000; pp 211–220; (b) Warmuth, R.; Yoon, J. *Acc. Chem. Res.* **2001**, *34*, 95–105; (c) Liu, Y.; Warmuth, R. *Org. Lett.* **2007**, *9*, 2883–2886.
18. Del Piero, S.; Fedele, R.; Melchior, A.; Portanova, R.; Tolazzi, M.; Zangrando, E. *Inorg. Chem.* **2007**, *46*, 4683–4691.
19. Shivanyuk, A.; Rebek, J., Jr. *Chem. Commun.* **2002**, 2326–2327.
20. (a) Halper, S. R.; Do, L.; Stork, J. R.; Cohen, S. M. *J. Am. Chem. Soc.* **2006**, *128*, 15255–15268; (b) Rasika Dias, H. V.; Jin, W. *J. Am. Chem. Soc.* **1995**, *117*, 11381–11382.
21. Crystal data for **3** (the crystals were grown from $CDCl_3$ by slow evaporation at 298 K; CCDC 683966): $C_{57}H_{36}N_6O_6\cdot CDCl_3$, MW=1021.29, triclinic, *P*-1 (No. 2), a=14.0862(1) Å, b=14.1441(1) Å, c=14.4437(1) Å, α=68.785(1)°, β=70.046(1)°, γ=72.015(1)°, V=2464.63(3) Å^3, Mo Kα radiation, T=150 K, Z=2. 54,852 reflections measured, 8650 unique reflections (R_{int}=0.039), $R_1(F)$ for $I>2\sigma(I)$ was 0.049 and $wR_2(F^2)$ for all data was 0.150. The asymmetric unit consists of the basket-shaped molecule with a molecule of $CDCl_3$ inside its cavity. There is also a region of disordered electron density located outside of the basket-shaped molecule and about an inversion center. This is most likely a disordered solvent molecule and since a reasonable model could not be obtained for this region, the SQUEEZE procedure[22] of PLATON[23] was used to account for the electron density in this region. The total solvent accessible void is 165 Å^3 and the electron count for this region is 27 electrons/unit cell.
22. Sluis, P. V. D.; Spek, A. L. *Acta Crystallogr.* **1990**, *A46*, 194–201.
23. (a) Spek, A. L. *Acta Crystallogr.* **1990**, *A46*, C34; (b) Spek, A. L. *A Multipurpose Crystallographic Tool, PLATON*; Utrecht University: Utrecht, The Netherlands, 1998.
24. Crystal data for **2** (the crystals were grown from CD_2Cl_2/CD_3OD by slow evaporation at 298 K; CCDC 683968): $C_{57}H_{36}N_6O_6$, MW=900.92, trigonal, *R*-3 (No. 148) on hexagonal axes, a=16.7213(2) Å, c=30.3229(4) Å, V=7342.4(2) Å^3, Mo Kα radiation, T=150 K, Z=6. 49,686 reflections measured, 2880 unique reflections (R_{int}=0.037), $R_1(F)$ for $I>2\sigma(I)$ was 0.049 and $wR_2(F^2)$ for all data was 0.146. The asymmetric unit consists of a basket-shaped molecule on a crystallographic threefold rotation axis with a disordered solvent molecule inside its cavity. There is also a region of disordered electron density located outside of the basket-shaped molecule. Since a reasonable model could not be obtained for the disordered regions, the SQUEEZE procedure[22] of PLATON[23] was used to account for the electron density in these regions. The total solvent accessible void is 1267 Å^3 and the electron count for this region is 285 electrons/unit cell.
25. Crystal data for **4** (the crystals were grown from $CDCl_3$ by slow evaporation at 298 K; CCDC 683967): $C_{57}H_{36}N_6O_6\cdot CH_3OH\cdot H_2O$, MW=950.98, trigonal, *R*-3 (No. 148) on hexagonal axes, a=16.2968(1) Å, c=32.3226(4) Å, V=7434.3(1) Å^3, Mo Kα radiation, T=150 K, Z=6. 50,906 reflections measured, 2921 unique reflections (R_{int}=0.040), R_1(F) for $I>2\sigma(I)$ was 0.082 and $wR_2(F^2)$ for all data was 0.265. The basket-shaped molecule contains a crystallographic threefold rotation axis. Inside this molecule is a disordered region of electron density, which was modeled in terms of a methanol and a water molecule. The water molecule sits on the threefold axis and the methanol molecule is disordered about the threefold axis. So for every water molecule inside the basket, there appears to be one methanol molecule. The carbon atom of the methanol seems to be disordered over two sites: C(20A) and C(20B). There is a second region of disordered electron density located outside of the basket molecule. This is most likely to be another disordered methanol and/or water molecule. The SQUEEZE procedure[22] of PLATON[23] was used to account for this disordered solvent region. The total solvent accessible void is 533 Å^3 and the electron count for this region is 56 electrons/unit cell.
26. Meyer, E. A.; Castellano, R. K.; Diederich, F. *Angew. Chem., Int. Ed.* **2003**, *42*, 1210–1250.
27. Dalgarno, S. J.; Antesberger, J.; McKinlay, R. M.; Atwood, J. L. *Chem.—Eur. J.* **2007**, *13*, 8248–8255.
28. Rieth, S.; Baddeley, C.; Badjić, J. D. *Soft Matter* **2007**, *3*, 137–154.
29. Hunter, C. A. *Angew. Chem., Int. Ed.* **2004**, *43*, 5310–5324.